ADSORPTION MEASUREMENTS IN DEVONIAN SHALES

X. Lu, F.C. Li, and A.T. Watson

Department of Chemical Engineering

Texas A&M University

Abstract

The Devonian shales in the Appalachian basin are considered a major potential source of future domestic natural gas. In these formations, natural gas is believed to be stored as conventional "free" gas in porous spaces as well as "adsorbed" gas on shale matrix. Studies have suggested that more than half of the total gas storage in the Devonian shales exists as an adsorbed state. Despite the importance of gas adsorption in Devonian shales, measurements of adsorption isotherms are scarce due to the difficulties associated with gas-shale systems. In this study, experimental methodologies have been developed for accurate gas-shale adsorption measurement at different temperatures. To ensure the accuracy of the measurements, emphasis is placed on developing laboratory procedures that ensure accurate cell calibration and precise temperature control. Detailed error analyses have been performed to guide the apparatus design. Methane isotherms on various shale samples have been measured, the gas storage mechanisms of Devonian shales are investigated, and various factors which would affect the gas-shale adsorption are elucidated.

Introduction

Large amounts of natural gas accumulations exist in the Devonian shale formation of the Appalachian, Michigan, and Illinois basins. It is estimated that several thousand trillion cubic feet (Tcf) of gas are contained in this area [1]. These Devonian shales are a major potential source of future domestic natural gas. The gas storage mechanisms in Devonian shales are quite different from those in conventional gas reservoirs. In the Devonian shales, natural gas is believed to be stored as conventional "free" gas in the porous space as well as a condensed phase on the shale matrix and organic materials. Some studies suggest that more than 50% of the total gas storage in the Devonian shales exist as a condensed phase [2-4]. The condensed phase gas storage includes the adsorbed gas on shale surfaces and soluted gas in organic materials. Certain types of clay minerals and the organic kerogen in the Devonian shales are the main components believed to be responsible for condensed phase gas storage. We will use the term "adsorbed gas" to refer the condensed phase gas since the measured adsorption isotherm includes all the condensed phase.

The importance of gas adsorption in Devonian shales has been revealed in the studies of Lane *et al.* [5,6]. They indicated that when adsorbed gas is present in the shales, production forecasts that include the effects of gas adsorption are often far more accurate than when adsorption is not taken into account. Another consideration is that the prediction of the effects of stimulation efforts can be significantly affected by the manner in which gas is stored. For example, raising

the temperature of the reservoir can greatly enhance the production rate when there is significant storage by adsorption; if gas were stored just in the conventional manner, there would be relatively little enhancement [6]. Lane *et al.* [5,6] determined that adsorption generally cannot be determined accurately from history matching production data alone. While they proposed a specific well-test design to determine adsorption from reservoir data [7], the method has not yet been demonstrated in the field. The testing of actual shale samples from core samples is necessary for characterizing adsorption in Devonian shales.

Measurements of adsorption isotherms for Devonian shale samples have not been widely available. Even though the adsorption mechanism is clearly important in the shales, the adsorption capacity is considerably less than adsorbents typically of interest in adsorption studies. The measurement errors which can be tolerated with other adsorbents would invalidate the results for Devonian shales. Consider, for example, adsorption of methane gas, the major component of natural gas. At room temperature and about 1,000 psi pressure, the methane adsorption capacities of Devonian shales are around 0.5 – 5.0 standard cubic centimeter per gram sample (scc/gram) [2-4]. At the same conditions, the methane adsorption capacity of activated carbons is about 120 scc/gram [8]; that for zeolite is about 100 scc/gram [9]; and that for coals is about 25 scc/gram [10]. There is more than an order of magnitude difference in the methane adsorption capacities between Devonian shales and other conventional adsorbents. If an apparatus can measure adsorption isotherms for zeolite within 5 % error, the same apparatus would give more than 100 % errors for measurements on Devonian shales, which clearly would invalidate the measurement results. This observation, coupled with the fact that relatively small amounts of sample may be available for such tests, means that many of the standard laboratory methods are not suitable for work with Devonian shales.

In this paper we report on a laboratory apparatus and experimental methodology for measuring gas adsorption in Devonian shales accurately at high pressures and at various temperatures on Devonian shales. To ensure the accuracy of the measurement, particular attention is given to the development of laboratory procedures for accurate cell calibration and precise temperature control. We also investigate gas storage mechanisms on various Devonian shale samples, and elucidate various factors which will affect adsorption of gas in shales.

Volumetric Adsorption Measurements

Isotherm Calculation

In this study, a volumetric adsorption apparatus was designed and constructed for gas-shale isotherm measurements. The main parts of the apparatus are the reference cell and the sample cell as shown in Figure 1. During the isotherm measurement, a certain amount of gas is charged into the reference cell. After equilibrium is reached, the valve between the cells is opened, and the gas is expanded into the sample cell. By measuring the pressures and temperatures before and after gas expansion, the gas molar densities at different stages can be calculated with an appropriate equation of state (EOS); then the amount of gas adsorbed at one pressure level can be calculated. By increasing the amount of gas charged into the reference cell, and repeating the same procedures, the amount of adsorbed gas at another pressure level can be obtained. The isotherm is obtained by repeating these procedures until the measurement at the highest desired gas pressure is achieved.

Two types of isotherms, the adsorption isotherm and total sorption isotherm, have been measured. The adsorption isotherm, $N_{ads}(P)$, is the relationship between the amount of adsorbed gas and the gas pressure. The total sorption isotherms, $N_{sorb}(P)$, is the relationship between the

total amount of sorbed gas, which is the sum of the adsorbed gas and the "free" gas stored inside the sample pore volume, and the gas pressure. In order to measure these two isotherms, two gases, helium and methane, are used. First, the isotherm measurement with helium gas is performed. This experimental run serves the purpose of measuring the void volume. The void volume is defined as the total "free" volume that helium gas can penetrate when the sample is present inside the sample cell. Since helium gas is virtually non-adsorbable at room temperature, we can assume that no helium gas will be adsorbed on the sample when helium gas is expanded from reference cell to sample cell. Assuming that the adsorption isotherm is measured at n pressure levels, we have for the i-th pressure level:

$$V_{void}(i)\rho_e(i) = V_{ref}\sum_{j=1}^{i}[\rho_c(j) - \rho_e(j)] \quad i = 1, 2, \ldots, n \quad \text{for} \quad \text{helium} \tag{1}$$

where i refers to for the i-th pressure level, ρ is the gas molar density calculated at measured pressure and temperature. The subscripts c and e stand for charging and equilibrium, respectively, V_{ref} is the reference cell volume, and V_{void} is the void volume. With the knowledge of void volume, sample cell volume, V_{cell}, and bulk sample volume, V_{sample}, the sample porosity, ϕ, can be calculated:

$$\phi = \frac{V_{void} - V_{cell}}{V_{sample}}$$

where V_{cell} is the sample cell volume, and V_{sample} is the bulk sample volume.

Next, the isotherm measurement with methane is performed. Since methane gas is the major component of natural gas, it is expected that the isotherms measured with methane gas are representative of those of natural gas.

For the measurement of the adsorption isotherm, the amount of adsorbed gas at pressure P is given by:

$$N_{ads}(P) = N_{total}(P) - N_{ref}(P) - N_{void}(P) \tag{2}$$

where $N_{total}(P)$ is the total amount of gas charged into the reference cell over the course of the experiment, $N_{ref}(P)$ is the amount of gas remaining inside the reference cell at equilibrium, and $N_{void}(P)$ is the amount of gas filling the void volume. At the i-th pressure level, Eq. 2 can be written as:

$$N_{ads}(i) = V_{ref}\sum_{j=1}^{i}[\rho_c(j) - \rho_e(j)] - V_{void}\rho_e(i) \quad i = 1, 2, \ldots, n \tag{3}$$

For the measurement of the total sorption isotherm, the amount of gas sorbed by the sample at pressure P is given by

$$N_{sorb}(P) = N_{total}(P) - N_{ref}(P) - N_{cell-sample}(P) \tag{4}$$

where $N_{cell-sample}$ is the amount of "free" gas contained in the volume which is the sample cell volume less the bulk sample volume. At i-th pressure level, Eq. 4 can be written as:

$$N_{sorb}(i) = V_{ref}\sum_{j=1}^{i}[\rho_c(j) - \rho_e(j)] - (V_{cell} - V_{sample})\rho_e(i) \quad i = 1, 2, \ldots n \tag{5}$$

Equations 1, 3, and 5 are the main equations used to calculate the isotherms in the volumetric isotherm measurement.

Error Analysis

Due to the relatively small amount of sample material generally available, and the relatively small adsorptive capacity, the accuracy of the estimation of the amount of gas adsorbed becomes a crucial issue. To our knowledge, no systematic error analysis for a volumetric adsorption apparatus has ever been reported. By performing an error analysis, factors which will affect the measurement accuracies can be identified, and the apparatus can be designed to achieve accurate isotherm measurements.

For a volumetric adsorption measurement, the primary errors arise from the errors of the pressure and temperature measurements, ΔP and ΔT, and the error of the empirical equation of state (EOS). All three primary errors contribute to the over all measurement error via gas density calculations. The total error in gas density calculations from an EOS, $\Delta\rho$, based on measured pressure P and temperature T, can be expressed as:

$$\Delta\rho = \Delta\rho_{\mathrm{EOS}} + \frac{\partial\rho_{\mathrm{EOS}}}{\partial T}\Delta T + \frac{\partial\rho_{\mathrm{EOS}}}{\partial P}\Delta P \tag{6}$$

Here $\Delta\rho_{EOS}$ is the error of the EOS. The functional forms of EOS, ρ_{EOS}(P,T), are quite complicated for most of the practical EOS's. We will apply the simplest EOS —the ideal gas law— to describe the temperature and pressure dependence of the molar densities since any empirical EOS has similar temperature and pressure effects. By doing so, Eq. 6 can be written as

$$\frac{\Delta\rho}{\rho} = \frac{\Delta\rho_{\mathrm{EOS}}}{\rho} + \frac{\Delta T}{T} + \frac{\Delta P}{P} \tag{7}$$

The first term on the right-hand-side accounts for errors arising from the EOS, and the second and third terms account for errors caused by temperature and pressure measurement errors, respectively. There are numerous published studies on equations of state for various gases [11-14]. We chose the most recently published EOS's for our experiments [12,13]. From the literature, the error for the equation of state of helium gas is 0.03 %, and that for methane gas is 0.02 % .

The other primary errors arise from the cell volume calibrations ΔV_{ref} and ΔV_{cell}, and the sample bulk volume measurement ΔV_{sample}. Table 1 lists the primary errors and their magnitudes encountered in our measurements.

The overall measurement errors associated with the adsorption isotherm, total sorption isotherm, and void volume can be estimated based on the Eqs. 1, 3, and 5. Details of the mathematical derivations are shown in Appendix.

Computer simulations of measurement errors were performed based on the equations governing the overall measurement errors (see Appendix). During the simulation, linear isotherms and the ideal gas law for gas density were assumed for simplicity. The inequality signs in those equations were replaced with equalities, so that simulated errors correspond to the maximum possible errors; we expect that the actual errors encounted during measurement will be smaller than that. During the simulation, cell volumes and sample volume used in our apparatus, which was designed with the guidance of the error analysis, were used. The design was based on a typical sample size of about 18 cc. This necessitates a sample cell size of about 25 cc after allowing for tubing and fittings.

The computer simulations revealed that selection of reference cell and sample cell volumes can strongly affect the measurement errors. This is explored in Figures 2a and 2b. It can be seen that the measurement accuracy increases when the ratio of reference cell volume to total cell volume decreases, or the ratio of sample volume to total cell volume increases. Here the total cell volume is the sum of reference cell volume and sample cell volume. Basically, it is desirable to

use as small a reference cell as is possible. This will result in the most accurate determination of the amount of gas charged into the system. Of course, this cell must be sufficiently large so that the pressure measurements are within the range of the pressure transducer. It is also desirable that the sample cell be filled to the fullest extent possible during the measurement.

The simulations shown that overall measurement errors can be reduced by reducing magnitudes of primary errors, as expected. For example, figures 2c and 2d show the dependence of measurement error on the error of reference cell volume calibration, ΔV_{ref}, and on the error of temperature measurement, ΔT. It can be see that the dependencies are almost linear. Therefore, reducing primary errors, such as improving the cell calibration accuracy and increasing the precision of temperature control, can effectively reduce the measurement errors.

The simulations also show that sufficient accuracy of isotherm measurement on low adsorption capacity adsorbents such as Devonian shale can be achieved with a carefully designed volumetric adsorption apparatus. Using the parameters listed in Table 1, the simulation results show that, in our apparatus, the percentage errors for both adsorption isotherm and total sorption isotherm measurements are less than 8%, as shown in Table 2. The typical shale adsorption capacity, 5.69 (scf/ft^3) or 2.4 (cc/gram) at 1000 psi, was assumed in this case.

Apparatus

Figure 3 shows the schematic diagram of the volumetric adsorption measurement apparatus. The design of the apparatus was guided with the results of the error analysis. The combination of various volumes was carefully selected. The reference cell (4.86cc) is much smaller than sample cell (25 cc) to ensure smaller measurement errors. In this cell combination, the maximum gas pressure encounted during the isotherm measurements is less than 2,000 psi, which is within the operating range of our pressure transducer. The volumes of tubing and fittings associated with the sample cell which are not filled by the samples were kept as small as possible to ensure a relatively large ratio of V_{sample}/V_{total}. Precise temperature control was designed which can maintain the system temperature within ± 0.005 of set point. A piezoelectric type pressure transducer with nominal accuracy of 0.01% was used to measure system pressures. The sample cell and reference cell are constructed with stainless steel. The connection of the sample cell with the system is provided by a Swagelok VCR Metal Gasket Face Seal Fitting to provide easy assembly–disassembly. The VCR fitting can provide good seals under high pressures even after numerous assembly-disassembly processes. Entrainment of adsorbent in the cell during vacuum is prevented by employing a filter gasket between the conjunction of tubing and the VCR fitting. All tubings used in the apparatus are 0.635 cm o.d. (0.25 inch) with a thick wall 0.21 cm (0.083 inch) stainless steel. Swagelok tube fittings and Nupro "HB" series air actuated high pressure valves are used in this apparatus. The valve is chosen because of its durability under high pressures (up to 3500 psi) and high temperatures. A water bath is employed to provide a constant temperature environment for the system. All the valves, pressure transducers, and temperature control units are interfaced with a personal computer. The operation of the apparatus is fully automatic.

Cell Calibration

As revealed by the error analysis, the accuracy of the cell volume calibration will strongly affect the accuracy of the adsorption measurement. In the conventional calibration methods, a liquid (distilled water or mercury) is used for the calibration of one of the cell volumes, or part of the apparatus volume, and the remaining volume is calibrated by filling the volume with a known amount of a non-adsorbing gas, usually helium [10,15,16]. The accuracy of this method is limited

for several reasons. First, due to the complex volume structure caused by fittings and valves, there may exist some spaces which the liquid can not invade. There may also be air bubbles in the liquid. Finally, there are errors associated with reading the amount of liquid entering the cell. There is no quantitative method to estimate the total error for this cell volume calibration method. By our experience, 1% to 2% calibration error is possible. As shown in Figure 2b, large measurement errors will occur with such calibration errors.

To achieve high accuracy in the cell volume calibration, we used a dual-gas expansion method. In the first gas expansion, both cells are empty; in the second gas expansion, a volume standard is placed in the sample cell. The accuracy of this calibration method is highly dependent upon the accuracy of the volume standard. For this reason, we used silicon crystals obtained from the National Institute of Standards and Technology (NIST) as the volume standard. The density of the crystal was accurately measured (2.3289819 ± 0.0000014 gram/cc) [17]. The description of the calibration method follows.

The calibration consists of two gas expansion processes. In the first expansion, a certain amount of helium gas inside reference cell at pressure P_c is expanded into the sample cell. When equilibrium is reached, the system pressure P_e is measured. By a mass balance, we have:

$$V_{cell} = V_{ref}\frac{\rho(P_c) - \rho(P_e)}{\rho(P_e)} \tag{8}$$

Here $\rho(P_c)$ and $\rho(P_e)$ are the gas molar densities at charging and equilibrium gas pressures, respectively. In the second gas expansion, the silicon crystal (NIST volume standard) is loaded into the sample cell, and the same procedures as the first expansion are followed. Again, by mass balance, we have:

$$V_{cell} - V_{standard} = V_{ref}\frac{\rho(P_c^*) - \rho(P_e^*)}{\rho(P_e^*)} \tag{9}$$

Here $V_{standard}$ is the volume of crystals in the sample cell, and $\rho(P_c^*)$ and $\rho(P_e^*)$ are the gas molar densities at charging and equilibrium pressures, respectively. There are two unknows in Eqs. 8 and 9, V_{cell} and V_{ref}. Solving these two equations simultaneously, we get the reference cell volume:

$$V_{ref} = V_{standard} / \left[\frac{\rho(P_c) - \rho(P_e)}{\rho(P_e)} - \frac{\rho(P_c^*) - \rho(P_e^*)}{\rho(P_e^*)}\right] \tag{10}$$

Substituting V_{ref} into Eq. 11, we can get the sample cell volume V_{cell}. It must be noted that all the calibration procedures are carried out at a constant temperature.

The error in this calibration method can be estimated as follows. From Eq. 13, the following equation can be derived:

$$\frac{\Delta V_{ref}}{V_{ref}} \leq \frac{\Delta V_{standard}}{V_{standard}} + \frac{V_{ref}}{V_{standard}}\left[\frac{\rho(P_c)}{\rho(P_e)}\left(\frac{\Delta\rho(P_c)}{\rho(P_c)} + \frac{\Delta\rho(P_e)}{\rho(P_e)}\right) + \frac{\rho(P_c^*)}{\rho(P_e^*)}\left(\frac{\Delta\rho(P_c^*)}{\rho(P_c^*)} + \frac{\Delta\rho(P_e^*)}{\rho(P_e^*)}\right)\right] \tag{11}$$

Since we used the NIST volume standard, the error of $\Delta V_{standard}/V_{standard}$ can be neglected. From Table 1, we know that the typical error for density calculation is less than 0.044% for helium gas. So the calibration error estimated by Eq. 14 is less than 0.4 %, which is much better than the conventional liquid filling method.

Temperature Control

Precise temperature control is crucial for accurate isotherm measurement. First, the variation of temperature during the experiment will cause errors in temperature measurement, ΔT. Second, the variation of the temperature will cause fluctuations of system pressures. According to the ideal gas law, variations in temperature of ± 0.1 at 25°C will cause gas pressure fluctuations of 0.6 psi at 1000 psi. For such large pressure fluctuations, the true equilibrium system pressure can not be accurately measured. Also, this pressure uncertainty will in turn cause additional measurement errors according to Eq. 7.

A electric heater with a proportional-integral (PI) controller was used to maintain the temperature at selected levels. The root-locus method [18] was used to select the controller gain, K_c, and integral time constant, τ_I, using the following model of the controller:

$$c(t) = K_c[T(t) - T_{set}] + \frac{K_c}{\tau_I}\int [T(t) - T_{set}]\, dt + c_s \tag{12}$$

where $T(t)$ is the measured system temperature, T_{set} is the set point temperature, and c_s is the controller's bias signal.

For that analysis, a model of the process is required. Assuming that the water is perfectly mixed, heat transfer to the surrounding air can be represented with a single overall heat transfer coefficient, and the heat capacity of the tank is negligible, an energy balance yields the following equation:

$$q - UA(T - T_\infty) = mc_p\frac{dT}{dt} \tag{13}$$

where m is the mass of water in the tank, q is the heat rate provided by the electric heater, c_p is the water heat capacity, U is the overall heat transfer coefficient between water and air, A is the total heat transfer area, and T_∞ is the temperature of surrounding air. By defining the time constant of the process, τ_p, and steady-state gain of the process, K_p, as follows:

$$\tau_p = mc_p/UA \tag{14}$$

$$K_p = 1/UA \tag{15}$$

Eq. 13 can be rewritten as:

$$qK_p - (T - T_\infty) = \tau_p\frac{dT}{dt} \tag{16}$$

Assuming a constant step input heat rate, $q = C_o$, the solution of Eq. (16) is:

$$T(t) = C_oK_p(1 - e^{-t/\tau_p}) + T_\infty \tag{17}$$

In order to obtain the process parameters K_p and τ_p, the temperature response to a series of input heat rates, C_o, were measured. A least squares procedure was used to obtain estimates of K_p and τ_p using Eq. 17. The measured data along with the predicted response obtained from the least-squares estimates are shown in Figure 4a. It can be seen that the simple model provides a reasonable, although not entirely accurate, representation of the process. Using the process model, the parameters for the controller model, τ_I and K_c, can be selected by the root-locus method [4].

Using this method, we achieved a temperature control to within ±0.005°C of the set point. The system temperature can be stabilized within a couple of hours after a change in set point as shown in Figure 4b.

Samples

The samples used in this study are from Gas Research Institute (GRI) sponsored Devonian shale study wells. The CSW samples are from wells in West Virginia and Kentucky, and the Antrim samples are from wells in Michigan. The illite sample, one of the major mineral components of Devonian shale, was acquired from Clay Mineral Society. The samples are crushed to 18-25 mesh size particles and degassed at 50-60°C for 24 hours in a vacuum oven prior to isotherm measurement. The samples are regenerated after each measurement by evacuation at 50°C overnight.

Results and Discussion

First, we checked the reproducibility of the adsorption measurements by running replicate experiments. As indicated before, two kinds of isotherms were measured for each sample, the adsorption isotherm and the total sorption isotherm. The adsorption isotherm accounts for the condensed gas storage, which includes adsorbed gas on shale surfaces and soluted gas in organic materials; the total sorption isotherm accounts for both condensed gas storage and "free" gas storage in porous spaces. Figure 5 shows the replicated measurement results for two shale samples. It is shown that reproducibilities of both adsorption isotherms and total sorption isotherms are good. The differences of repeated results are all within 3%. The good reproducibilities show the consistency and accuracy of the measurements.

Most of the Devonian shales have relatively small porosities, ranging from 1% to 8%. The ability of Devonian shale to hold significant amounts of natural gas is the result of condensed phase gas storage. To see the relative importance of adsorbed gas storage to total gas storage, isotherms were measured on twenty-four Devonian shale samples obtained from five different wells, and the ratios of the amount of adsorbed gas to the total storage at 500 psi pressure were calculated. The isotherm temperatures vary from sample to sample, ranging from 24°C to 37.78°C. It was found that, for a shale sample, this ratio did not change significantly with isotherm temperatures in this temperature range [4]. Figure 6 is a histogram of the ratios among twenty-four samples. The histogram indicates that for most of the samples, the ratio is larger than 50%, which means that adsorbed gas accounts for more than half of the total stored gas. The average ratio among these samples is 61%.

Since adsorption plays an important role in natural gas storage in Devonian shales, we may ask what factors are responsible for the adsorbed gas storage. Because significant organic materials exist in most Devonian shales, and the organic materials have significant solubilities of natural gas, the adsorbed gas may exists as a solution in the organic materials. It was found that in some Devonian shales with high organic material contents, there is a linear correlation between the adsorption isotherm slopes and the total organic carbon (TOC) [3]. The adsorption isotherm slope is related to the Henry's constant at very low gas pressures. To see the relationship between the adsorption capacities and the total organic carbon (TOC) present in the shales, the amount of adsorbed gas versus the total organic carbon [19] at two gas pressures for eight shale samples are plotted in Figure 7. Fairly good linear correlations between the adsorbed gas amount and TOC are observed in Figure 7, indicating that organic material is one of the important factors responsible for adsorbed gas storage. But, as one can see from Figure 7, shale samples with very

low organic carbon contents (less than 1% TOC) still have significant adsorbed gas storage. It suggests that some other minerals are responsible for the adsorbed gas storage. Since the main mineral compositions of Devonian shale are clay (mainly illite), carbonates and quartz [19], and since carbonates and quartz are non-adsorbable for natural gas, illite may be the other factor for the adsorbed gas storage. To verify this, adsorption isotherms were measured on an illite sample; the results are shown in Figure 8. It can be seen that the adsorption capacity of illite is significant compared with that of Devonian shales. There are about 10% to 40% weight percent of illite present in Devonian shales [19], and the adsorbed natural gas on illite can contribute significantly to the total gas storage in Devonian shales.

We also examined the temperature effect on the gas adsorption of Devonian shales by measuring the isotherms at different temperatures. This information is crucial for studies of thermal stimulation of gas reservoirs[6]. However, no measurements of gas-shale isotherms at multiple temperatures have ever been reported. We measured isotherms at temperatures ranging from 25°C to 60°C. Figure 9 shows measured results for two shale samples. The adsorption capacity of the shales increase as the temperature decreases, which is expected since gas adsorption on solids is an exothermic process. With the isotherms measured at multiple temperatures, quantities characterizing the gas-shale system, such as isosteric heat, maximum adsorption capacity and heterogeneities, can be quantified. Also, the mechanisms of adsorbed gas storage could be identified using carefully selected models, and adsorption isotherms at other temperatures can be predicted.

Conclusions

1. A detailed error analysis has been performed for the volumetric gas-shale adsorption apparatus, and various factors which would affect the accuracy of the measurement were identified. The analyses were used to guide the apparatus design.

2. A new cell volume calibration method using dual-gas expansion and NIST volume standard has been developed. The new calibration method resulted in much higher accuracies in the cell volume calibrations than the conventional liquid filling method.

3. A temperature control system has been designed so that the apparatus can be operated at selected temperatures. The high precision temperature control (± 0.005°C) is important for accurate adsorption measurements.

4. The results of adsorption measurements on twenty-four shale samples obtained from five wells have shown that more than half of the total gas storage in the Devonian shales exists in a condensed state.

5. A fairly linear correlation between adsorption capacities and total organic contents of shale samples has been observed, which indicates that gas solution on organic material is one of major mechanisms of adsorbed gas storage in shales.

6. Significant gas adsorption capacity on illite, which is one of the major mineral contents in shales, has been observed. Illite may be responsible for adsorbed gas storage in shale samples with very low organic content.

7. Adsorption isotherms at various temperatures have been measured. With these isotherm data, further studies of gas storage mechanisms and gas-shale thermodynamic properties can be performed.

Acknowledgement

The authors gratefully acknowledge the financial support of this work by the Gas Research Institute. The authors wish to acknowledge important contributions by Scott Lane, Chih-An Hwang, and Jim Holste in the early stages of this work, and many helpful discussions with Paul Schettler throughout the work.

Nomenclature

A	= heat transfer area (m^2)
c_p	= heat capacity (Joule/°K/gram)
$c(t)$	= actuating signal (Joule/sec)
c_s	= temperature controller's bias signal (Joule/sec)
C_o	= step input of heat rate (Joule/sec)
EOS	= equation of state
K	= steady-state gain (sec°K/Joule)
m	= mass of water in tank (kg)
N	= amount of gas (mole)
P	= adsorbate pressure (psi)
q	= heat rate (Joule/sec)
R	= gas constant (Joule/°K/mole)
T	= absolute temperature (°K)
T_∞	= absolute temperature of surrounding air (°K)
t	= time (sec)
U	= heat transfer coefficient (Joule/m^2/°K/sec)
V	= volume (m^3)

Greek

ϕ	= helium porosity (%)
ρ	= molar density (mole/m^3)
τ	= time constant (sec)

Subscript

ads	= adsorption
c	= charge
CH4	= methane gas
cell	= sample cell
e	= equilibrium
EOS	= equation of state
He	= helium gas
pore	= pore volume
ref	= reference cell
sample	= shale sample
set	= set point
sorb	= total sorption
total	= total amount of gas
void	= void volume

Reference

1. Smith, E.C., "A Practical Approach to Evaluating Shale Hydrocarbon Potential", *Second Eastern Gas Shale Symposium Preprints*, DOE/METC/SP–78/6, Vol. II 73 (1978).

2. Thomas, J. Jr., and Frost., R. R., "Adsorption/Desorption Studies of Gases through Shales", In *Geological and Geochemical Studies of the New Albany Shale Group (Devonian–Mississippian) in Illinois*, Eds. R. E. Bergstrom and N. F. Shimp, DOE/METC/12142-0026, (1980).

3. Schettler, P. D., and Parmely, C. R., "Contributions to Total Storage Capacity in Devonian Shales," paper SPE 23422, presented at the SPE Eastern Regional Meeting held in Lexington, Kentucky, October 22-25, (1991).

4. Li, F.C., *Methane Adsorption on Devonian Shales*, M.S. Thesis, Texas A&M University, December, 1992.

5. Lane, H. S., Lancaster, D. E., and Watson, A. T.,"Characterizing the Role of Desorption in Gas Production From Devonian Shales," *Energy Sources*, 13, 337 (1991).

6. Lane, H. S., Watson, A. T., and Lancaster, D. E., *Identifying and Estimating Desorption from Devonian Shale Gas Production Data*, S.A. Holditch and Associates, Inc., Topical Report to the Gas Research Institute, GRI-89/0205, (1989).

7. Watson, A.T., Gatens, J.M. III, and Lane, H.S., "Model Selection for Well Test and Production Data Analysis", SPE *Form. Eval.* 215 (Mar. 1988).

8. Rajiv, K.A. and Schwarz, J., "Analysis of High Pressure Adsorption of Gases on Activated Carbon by Potential Theory", *Carbon*, Vol. 26(6), 873(1988).

9. Zhang, S., Talu, O., and Hayhurst, D.T., "High Pressure Adsorption of Methane in Nax, MgX, CaX, SrX, and BaX Zeolite", *J. Phys. Chem.*, 95, 1722(1991).

10. Yang, R.T., Saunders, J.T., "Adsorption of Gases on Coals and Heat-treated Coals at Elevated Temperature and Pressure", *Fuel*, Vol. 64, 616(1985).

11. McCarty, Robert D., "Thermodynamic Properties of Helium 4 from 2 to 1500 K at Pressures to 10^8 Pa," *J. Phys. Chem. Data*, Vol. 2, No.4, 923 (1973).

12. Trappeniers, N.J., Wassenaar, T. and Abels, J. C.,"Isotherms and Thermodynamic Properties of Methane at Temperatures Between 0° and 150°C and at Densities up to 570 Amagat," *Physica* 98A, 289 (1979).

13. Angus, S., Armstrong, B. and de Reuck, K.M., *Helium—International Thermodynamic Tables of the Fluid State–4*, Pergamon Press, Oxford (1977).

14. Angus, S., Armstrong, B. and de Reuck, K.M., *Methane—International Thermodynamic Tables of the Fluid State–5*, Pergamon Press, Oxford (1978).

15. Ponec, V., Knor, Z., and Cerny, S., *Adsorption on Solids*, CRC Press, Cleveland, (1974).

16. Brunaur, S., *The Adsorption of Gases and Vapors*, Princeton University Press, Princeton, (1943).

17. Bowman, H.A., Schoonover, R.M., and Jones, M.W., "Procedure for High Precision Density Determinations by Hydrostatic Weighing," *Journal of Research of the National Bureau of Standard–C. Engineering and Instrumentation*, 71c, No. 3 (August 1967).

18. Stephanoponlos, G., *Chemical Process Control–An Introduction to Theory and Practices*, Prentice Hall, New Jersey (1984).

19. Guidry, F.K., Luffel, D.L., Olszewski, A.J., and Raymer, L.L., *"Formation Evaluation Technology for Production Enhancement"*, Restech Inc., Houston, Annual Technical Report to Gas Research Institute, GRI-90/0300, October (1990).

20. Shchigolev, B.M., *Mathematical Analysis of Observations*, Elsevier Publishing, New York, NY. (1965).

Appendix

Based on the Eqs. 1, 3, and 5, the errors associated with the measurements of adsorption isotherm, $\Delta N_{ads}(i)$, total sorption isotherm, $\Delta N_{sorb}(i)$, and void volume, $\Delta V_{void}(i)$, can be estimated according to the theory of error analysis [20]:

$$\begin{aligned}\Delta N_{ads}(i) &\leq \frac{\partial N_{ads}}{\partial V_{ref}}\Delta V_{ref} + \sum_{j=1}^{i}\frac{\partial N_{ads}}{\partial \rho_c(j)}\Delta\rho_c(j) + \sum_{j=1}^{i}\frac{\partial N_{ads}}{\partial \rho_e(j)}\Delta\rho_e(j) + \frac{\partial N_{ads}}{\partial V_{void}(i)}\Delta V_{void}(i) \\ &\leq \Delta V_{ref}\sum_{j=1}^{i}[\rho_c(j)-\rho_e(j)] + V_{ref}\sum_{j=1}^{i}[\Delta\rho_c(j)+\Delta\rho_e(j)] \\ &\quad + \Delta V_{void}(i)\rho_e(i) + V_{void}(i)\Delta\rho_e(i)\end{aligned}$$

$$\begin{aligned}\Delta N_{sorb}(i) &\leq \frac{\partial N_{sorb}}{\partial V_{ref}}\Delta V_{ref} + \sum_{j=1}^{i}\frac{\partial N_{sorb}}{\partial \rho_c(j)}\Delta\rho_c(j) + \sum_{j=1}^{i}\frac{\partial N_{sorb}}{\partial \rho_e(j)}\Delta\rho_e(j) \\ &\quad + \frac{\partial N_{sorb}}{\partial V_{cell}}\Delta V_{cell} + \frac{\partial N_{sorb}}{\partial V_{sample}}\Delta V_{sample} \\ &\leq \Delta V_{ref}\sum_{j=1}^{i}[\rho_c(j)-\rho_e(j)] + V_{ref}\sum_{j=1}^{i}[\Delta\rho_c(j)+\Delta\rho_e(j)] \\ &\quad + (\Delta V_{cell}+\Delta V_{sample})\rho_e(i) + (V_{cell}-V_{sample})\Delta\rho_e(i)\end{aligned}$$

$$\begin{aligned}\frac{\Delta V_{void}(i)}{V_{void}(i)} &\leq \left[\frac{\partial V_{void}(i)}{\partial V_{ref}}\Delta V_{void}(i) + \sum_{j=1}^{i}\frac{\partial V_{void}}{\partial \rho_c(j)}\Delta\rho_c(j) + \sum_{j=1}^{i}\frac{\partial V_{void}}{\partial \rho_e(j)}\Delta\rho_e(j)\right]/V_{void}(i) \\ &\leq \frac{\Delta V_{ref}(i)}{V_{ref}} + \frac{\sum_{j=1}^{i}[\Delta\rho_c(j)+\Delta\rho_e(j)]}{\sum_{j=1}^{i}[\rho_c(j)-\rho_e(j)]} + \frac{\Delta\rho_e(i)}{\rho_e(i)}\end{aligned}$$

These are the equations describing the errors in a volumetric adsorption measurement.

Table 1. Primary errors and the magnitudes

Error Sources	Typical Value	Magnitude (%)
Reference Cell, V_{ref} (cc)	4.86	0.40
Sample Cell, V_{cell} (cc)	13.0 and 25.0	0.40
Sample, V_{sample} (cc)	7.0 and 19.0	0.20
Temperature, T (°K)	295 to 343	0.0034
Pressure, P (psi)	100 to 1200	0.01
Helium EOS		0.03
Methane EOS		0.02
Helium Density, ρ_{He} (mole/lt)	0.3 to 4.0	0.044
Methane Density, ρ_{CH_4} (mole/lt)	0.3 to 4.0	0.034

Table 2. Error analysis for volumetric adsorption apparatus

Reference Cell Volume:	4.86 cc	Porosity:	5.00%
Sample Cell Volume:	25.0 cc	$V_{ref}/(V_{ref}+V_{cell})$:	16.28%
Sample Volume:	18.0 cc	$V_{sample}/(V_{ref}+V_{cell})$:	60.28 %

Pressure (psi)	N_{sorb} (scf/ft^3)	N_{ads} (scf/ft^3)	$\Delta N_{sorb}/N_{sorb}$ (%)	$\Delta N_{ads}/N_{ads}$ (%)
100	0.88	0.57	7.13	4.12
200	1.75	1.14	7.19	4.29
300	2.63	1.71	7.25	4.45
400	3.50	2.28	7.32	4.61
500	4.38	2.84	7.38	4.78
600	5.25	3.41	7.45	4.94
700	6.13	3.98	7.51	5.10
800	7.00	4.55	7.58	5.26
900	7.88	5.12	7.64	5.43
1000	8.75	5.69	7.70	5.59

Figures

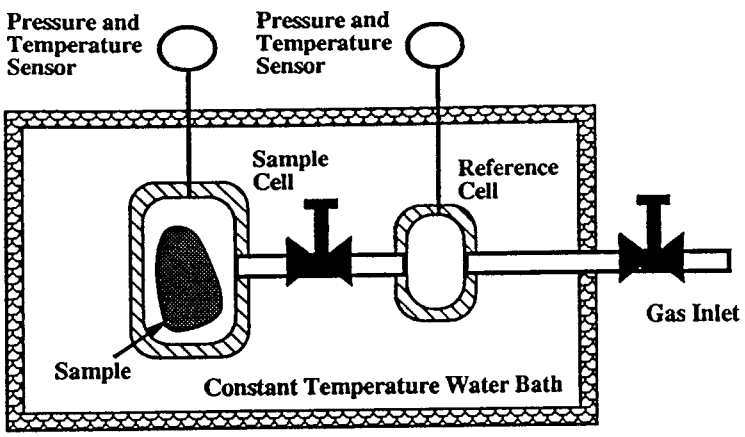

Figure 1. Schematic Diagram of Volumetric Adsorption Measurement Method

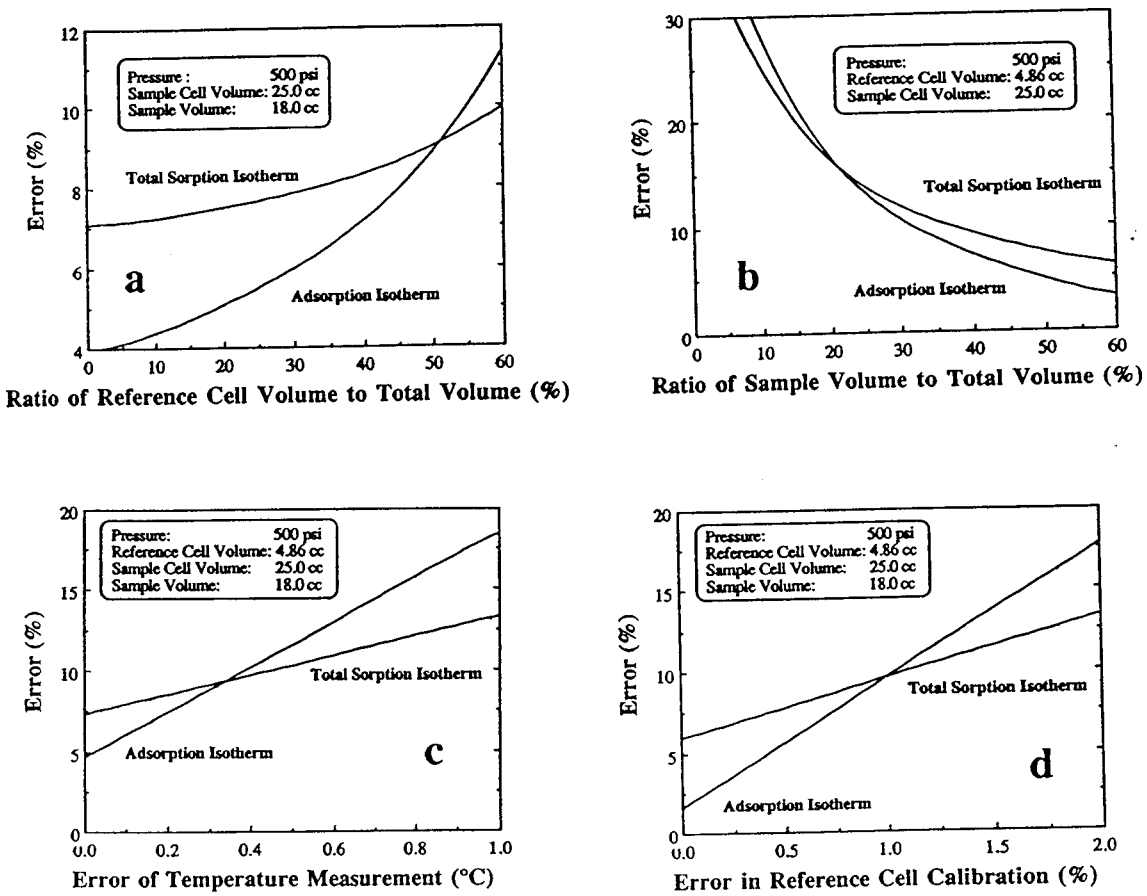

Figure 2. Dependence of Measurement Errors on Primary Errors

Figures

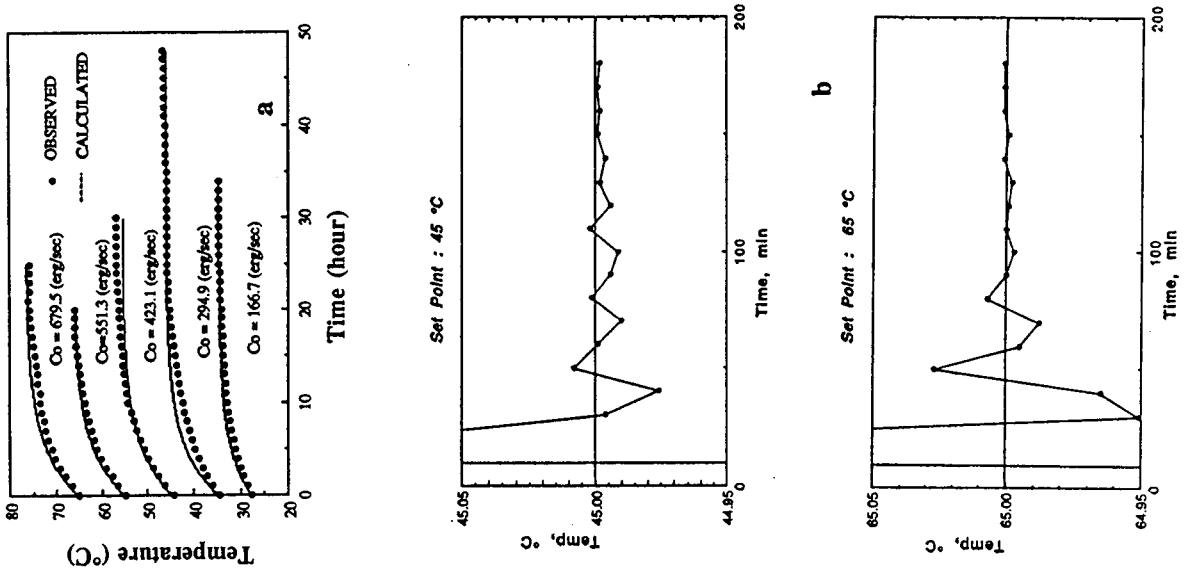

Figure 4. Temperature Contol of Water Bath

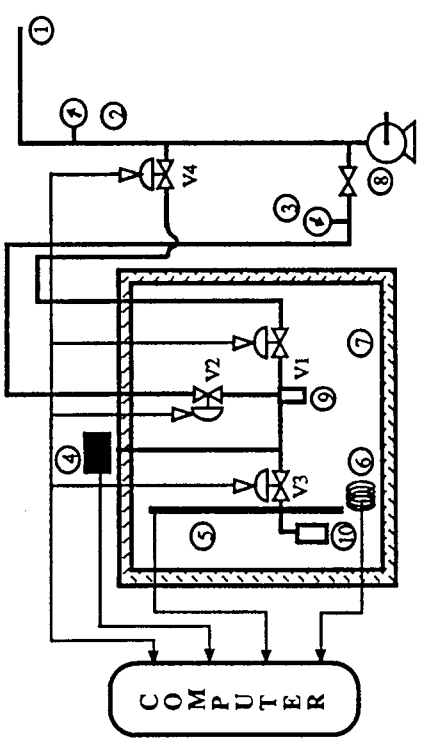

1. Gas Inlet
2. High Pressure Gauge
3. Low Pressure Gauge
4. Pressure Transducer
5. Thermometer
6. Heater
7. Water Tank
8. Vacuum Pump
9. Reference Cell
10. Sample Cell

Figure 3. Schematic Diagram of the Adsorption Apparatus

Figures

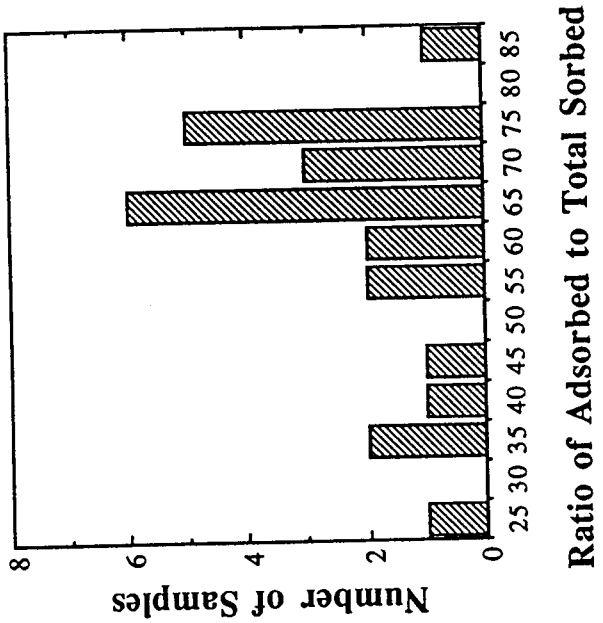

Figure 6. Histogram of Ratio of Adsorbed Gas Amount to Total Stored Gas Amount

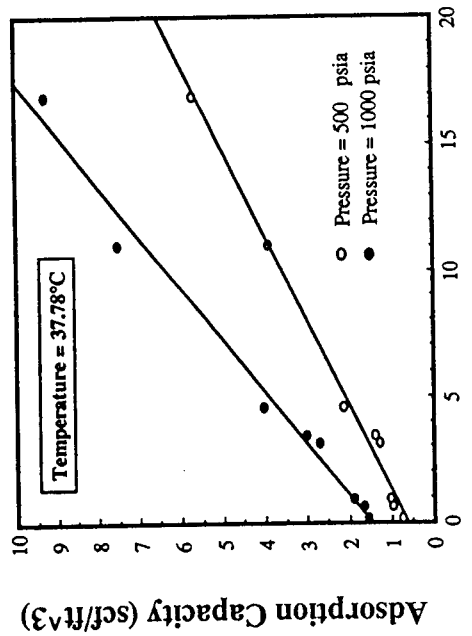

Figure 7. Raletionship between Adsorption Capacity and Total Organic Carbons

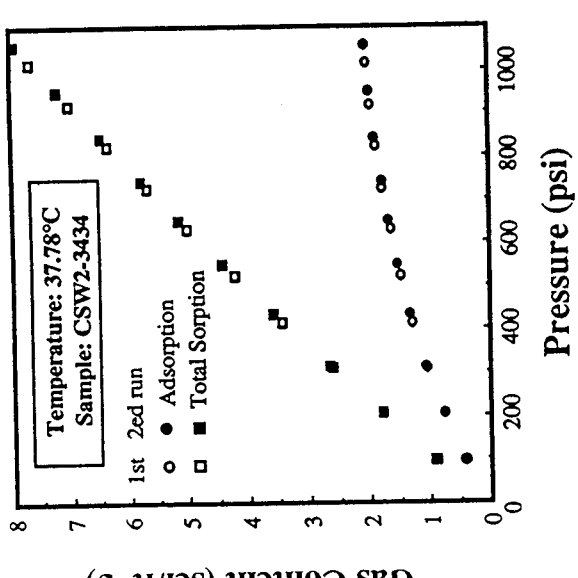

Figure 5. Replicated Measurements of Adsorption Isotherm and Total Sorption Isotherm

Figures

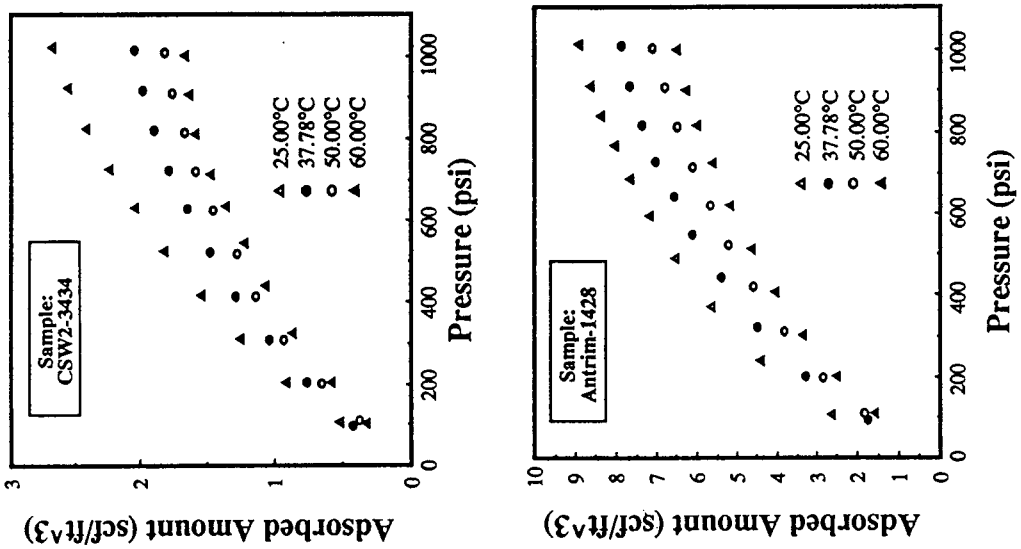

Figure 9. Adsorption Isotherms Measured at Various Temperatures

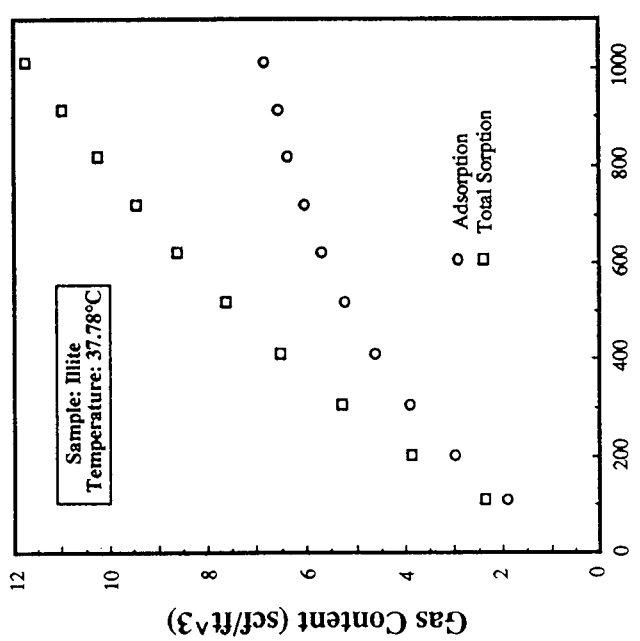

Figure 8. Adsorption and Total Sorption Isotherms of Illite

Captions

Figure 1. Schematic Diagram of Volumetric Adsorption Measurement Method

Figure 2. Dependence of Measurement Errors on Primary Errors

Figure 3. Schematic Diagram of Adsorption Apparatus

Figure 4. Temperature Control of Water Bath

Figure 5. Replicated Measurements of Adsorption Isotherm and Total Sorption Isotherm

Figure 6. Histogram of Ratio of Adsorbed Gas to Total Stored Gas

Figure 7. Relationship Between Adsorption Capacity and Total Organic Carbon

Figure 8. Adsorption and Total Sorption Isotherms of Illite

Figure 9. Adsorption Isotherms Measured at Various Temperatures